The Fluid-Solid Interaction of Cylindrical Structures—a Computer Oriented Approach

J. Stabel
Abt. B 112
Rott
Abt. R 152
Kraftwerk Union AG, Postfach 3220, D-8520 Erlangen, Germany

Summary

Analysis of the motional behaviour of two concentric cylinders separated by a fluid-filled gap requires adequate modeling of the fluid. For this purpose, a potential flow is generally postulated. If the motion of the two cylindrical structures is represented by the motion of a total of N discrete points, the interactive mechanisms induced by the fluid can be modeled by means of an N x N mass matrix (normally fully occupied). The matrix is represented in such a way that it can be readily implemented on existing computer programs.

1. Introduction

Structures which consist of 2 concentric cylinders separated by a fluid-filled gap are encountered relatively frequently in reactor engineering (cf. control rod/guide thimble, core barrel/RPV). It is known that their dynamic behaviour is strongly affected by interaction with the fluid. Natural frequency reductions to, for example, one third of the value in air are no rarity.

Postulating an ideal, incompressible, non-rotational fluid, it is possible to describe the interactive mechanisms with the aid of potential theory. It transpires that the interaction can be modeled by inclusion of an additional mass matrix, the hydromatrix, in the equation of motion.

The hydromatrix corresponding to the case of two infinitely long cylinders which move uniformly over their entire length is stated by Fritz /1/ (→ 2 x 2 matrix). The hydromatrix for the case of a stationary outer cylinder and a uniformly mobile inner cylinder of finite length is stated by Kiss /2/ (→ 1 x 1 matrix). In the present paper, the hydromatrix for the case of two cylinders of finite length which are capable of differing motion over their entire lengths is derived. If the movement of the inner and outer cylinders are represented by $\overline{K_1}$ and $\overline{K_2}$ points distributed over the length, the corresponding hydromatrix is a symmetric $(\overline{K_1} + \overline{K_2}) \times (\overline{K_1} + \overline{K_2})$ matrix which is generally fully occupied. It can readily be integrated into existing computer codes. In order to emphasize the differences to /1/, /2/ and /3/, this method is applied for the sake of example to the case of a stationary outer cylinder and a moving inner cylinder. Significant differences became apparent from mode 2 onwards (25 % difference in the 2nd eigenfrequency).

2. Derivation of the Additional Mass Matrix (Hydromatrix)

The system under analysis consists of 2 concentric cylinders (radius R_1 and R_2) separated by a gap filled with an ideal, incompressible, non-rotational fluid (fig. 1).

With $\underline{v}$ being the fluid velocity, we obtain

$$\nabla \wedge \underline{v} = \nabla \cdot \underline{v} = 0 \tag{1}$$

Therefore,

$$\exists\, \phi(R, \gamma, \varphi, t): \quad \underline{v} = -\nabla \phi \;, \quad \nabla^2 \phi = 0 \tag{2}$$

Let ϕ be:

$$\phi = \sum_{n=1,3,5,..}^{\infty} \left[E_n \cdot I_1(a_n R) + F_n \cdot K_1(a_n R) \right] \cos(a_n \gamma) \cdot \cos(\varphi) \tag{3}$$

where $E_n = E_n(t)$, $F_n = F_n(t)$, $a_n = \frac{n \cdot \pi}{2L}$

I_1, K_1 = modified Bessel function of the 1st and 2nd kind

Then we have:

$$\begin{aligned} &① \quad v_\gamma = 0 \quad \text{at} \quad \gamma = 0 \\ &② \quad p = \rho \frac{\partial \phi}{\partial t} = 0 \quad \text{at} \quad \gamma = L \\ &③ \quad v_R = -\frac{\partial \phi}{\partial R} = \frac{\partial w_i}{\partial t} \cdot \cos\varphi \quad \text{at} \quad R = R_i \quad (i = 1,2) \end{aligned} \tag{4}$$

It follows from ③ that (i = 1,2):

$$-\sum_{n=1,3,..}^{\infty} \left[E_n \cdot a_n \cdot I_1'(a_n R_i) + F_n \cdot a_n \cdot K_1'(a_n R_i) \right] \cdot \cos(a_n \gamma) \stackrel{!}{=} \frac{\partial w_i}{\partial t}(t, \gamma) \quad (i = 1,2) \tag{5}$$

It is to be borne in mind that $\{\cos(a_n \gamma)\}_{n = 1,3,5..}$ is complete on $[0, L]$.

After multiplication by $\cos(a_N \gamma)$ and integration from 0 to L it follows that:

$$E_N \cdot a_N \cdot I_1'(a_N R_i) + F_N \cdot a_N \cdot K_1'(a_N R_i) = -\frac{2}{L} \int_0^L \frac{\partial w_i}{\partial t} \cos(a_N \gamma)\, d\gamma \tag{6}$$

for i = 1,2 and N = 1,3,5,.....

For N = 1,3,.... and continuous functions f we formulate:

$$L_N(f) = -\frac{2}{L} \int_0^L f \cdot \cos(a_N \gamma)\, d\gamma \tag{7}$$

The following is then obtained for the pressure distribution p:

$$\begin{aligned} p = \rho \cdot \sum_{N=1,3,..}^{\infty} \Big[&\left(\gamma_{1,N} \cdot L_N\left(\frac{\partial^2 w_1}{\partial t^2}\right) + \gamma_{2,N} \cdot L_N\left(\frac{\partial^2 w_2}{\partial t^2}\right) \right) I_1(a_N R) + \left(\delta_{1,N} \cdot L_N\left(\frac{\partial^2 w_1}{\partial t^2}\right) \right. \\ &\left. + \delta_{2,N} \cdot L_N\left(\frac{\partial^2 w_2}{\partial t^2}\right) \right) K_1(a_N R) \Big] \cdot \cos(a_N \gamma) \cdot \cos\varphi \end{aligned} \tag{8}$$

where

$$\gamma_{1,N} = \frac{K_1'(a_N R_2)}{a_N \cdot \tau_N}, \quad \gamma_{2,N} = -\frac{K_1'(a_N R_1)}{a_N \cdot \tau_N}, \quad \delta_{1,N} = -\frac{I_1'(a_N R_2)}{a_N \cdot \tau_N}, \quad \delta_{2,N} = \frac{I_1'(a_N R_1)}{a_N \cdot \tau_N} \tag{9}$$

and

$$\tau_N = I_1'(a_N R_1) \cdot K_1'(a_N R_2) - I_1'(a_N R_2) \cdot K_1'(a_N R_1) \tag{10}$$

We approximate the functionals L_N by:

$$L_N\left(\frac{\partial^2 w_\gamma}{\partial t^2}\right) = \sum_{i=1}^{\overline{K_\gamma}} \varepsilon_{\gamma,i}^{(N)} \cdot \left(\frac{\partial^2 w_\gamma}{\partial t^2}\right)_i \quad (\gamma = 1,2) \tag{11}$$

where:

$\varepsilon_{\gamma,i}^{(N)}$ = Constant (see (19))

$\overline{K_1}$ = Number of points on inner cylinder

$\overline{K_2}$ = Number of points on outer cylinder

$(f)_i$ = Value of f at i^{th} point on inner or outer cylinder

Let

$$\lambda_i = \begin{cases} -1 , & i = 1 \\ 1 , & i = 2 \end{cases} \tag{12}$$

Then we have for the uniform loads P_1 and P_2 acting on the inner and outer cylinders respectively:

$$P_i(\gamma, t) = \lambda_i \, R_i \int_0^{2\pi} p(R_i, \gamma, \varphi) \cdot \cos\varphi \, d\varphi \quad (i = 1, 2) \tag{13}$$

with p from (8).

Then it follows with (11) that (i = 1,2):

$$P_i(\gamma,t) = \lambda_i \cdot \pi \cdot \rho \cdot R_i \sum_{N=1,3,\ldots}^{\infty} \sum_{I=1}^{\bar{K}_1} \sum_{J=1}^{\bar{K}_2} \left[\left(\gamma_{1,N} \cdot \varepsilon_{1,I}^{(N)} \left(\frac{\partial^2 w_1}{\partial t^2} \right)_I + \gamma_{2,N} \cdot \varepsilon_{2,J}^{(N)} \left(\frac{\partial^2 w_2}{\partial t^2} \right)_J \right) \cdot I_1(a_N R_i) + \left(\delta_{1,N} \cdot \varepsilon_{1,I}^{(N)} \left(\frac{\partial^2 w_1}{\partial t^2} \right)_I + \delta_{2,N} \cdot \varepsilon_{2,J}^{(N)} \left(\frac{\partial^2 w_2}{\partial t^2} \right)_J \right) \cdot K_1(a_N R_i) \right] \cdot \cos(a_N \gamma) \tag{14}$$

Integration over appropriate cylinder segments yields the following correlation between the nodal forces, the hydromatrix and the node accelerations:

$$\left[F_1, \ldots, F_{\bar{K}_1}, G_1, \ldots, G_{\bar{K}_2} \right]^T = - \underline{\underline{M}}_H \left[\left(\frac{\partial^2 w_1}{\partial t^2} \right)_1, \ldots, \left(\frac{\partial^2 w_1}{\partial t^2} \right)_{\bar{K}_1}, \left(\frac{\partial^2 w_2}{\partial t^2} \right)_1, \ldots, \left(\frac{\partial^2 w_2}{\partial t^2} \right)_{\bar{K}_2} \right]^T \tag{15}$$

where

$$\underline{\underline{M}}_H = \begin{pmatrix} \underline{\underline{M}}_{11} & \underline{\underline{M}}_{12} \\ \underline{\underline{M}}_{21} & \underline{\underline{M}}_{22} \end{pmatrix} \tag{16}$$

and

$$(M_{KL})_{IJ} = - \lambda_K \cdot \pi \rho R_K \cdot \left[\sum_{N=1,3,\ldots}^{\infty} \left(\gamma_{L,N} \cdot \varepsilon_{L,J}^{(N)} \cdot I_1(a_N R_K) + \delta_{L,N} \cdot \varepsilon_{L,J}^{(N)} \cdot K_1(a_N R_K) \right) \cdot \int_{\text{Seg. I,K}} \cos(a_N \gamma) \, d\gamma \right] \tag{17}$$

in which Seg. I, K (K = 1,2) are suibable cylindrical segments of the inner and outer cylinders respectively (see fig. 2, (19).

According to (7):

$$L_N(f) = - \frac{2}{L} \cdot \int_0^L f \cos(a_N \gamma) \, d\gamma \doteq - \frac{2}{L} \cdot \sum_{I=1}^{\bar{K}_P} \int_{\text{Seg I,P}} \cos(a_N \gamma) \, d\gamma \cdot f_I \tag{18}$$

where f_I is the "representative" value of f at Seg. I, P. This is the simplest possibility of approximating the functional L_N. It is evident then that:

$$\varepsilon_{P,I}^{(N)} = - \frac{2}{L} \cdot \int_{\text{Seg. I,P}} \cos(a_N \gamma) \, d\gamma \quad f. \; I = 1, \ldots, \bar{K}_P \; ; \; P = 1,2 \tag{19}$$

Let

$$S_{I,P}^{(N)} = \int_{\text{Seg I,P}} \cos(a_N \gamma) \, d\gamma \quad f. \; I = 1, \ldots, \bar{K}_P \; ; \; P = 1,2 \tag{20}$$

Then it follows for M_H from (16) that:

$$\begin{aligned} (M_{11})_{IJ} &= - \frac{2\pi\rho R_1}{L} \cdot \sum_{N=1,3,\ldots}^{\infty} \frac{S_{I,1}^{(N)} \cdot S_{J,1}^{(N)}}{a_N \cdot \tau_N} \left[I_1(a_N R_1) \cdot K_1'(a_N R_2) - K_1(a_N R_1) \cdot I_1'(a_N R_2) \right] \\ (M_{12})_{IJ} &= (M_{21})_{IJ} = - \frac{2\pi\rho}{L} \cdot \sum_{N=1,3,\ldots}^{\infty} \frac{S_{I,1}^{(N)} \cdot S_{J,2}^{(N)}}{a_N^2 \cdot \tau_N} \\ (M_{22})_{IJ} &= \frac{2\pi\rho R_2}{L} \cdot \sum_{N=1,3,\ldots}^{\infty} \frac{S_{I,2}^{(N)} \cdot S_{J,2}^{(N)}}{a_N \cdot \tau_N} \left[- K_1'(a_N R_1) \cdot I_1(a_N R_2) + I_1'(a_N R_1) \cdot K_1(a_N R_2) \right] \end{aligned} \tag{21}$$

$\underline{\underline{M}}_H$ is symmetrical and normally fully occupied. The asymptotic limit stated by Fritz in /1/ results for $L \to \infty$, $\bar{K}_1, \bar{K}_2 \to 1$.

3. Calculation Example

With reference to well-known structures in reactor engineering (cf. system of RPV/core barrel) we analyze the typical application of an oscillating system consisting of 2 concentric cylinders (fig. 3). The annular gap between the two cylinders is filled with a fluid, with both cylinders being coupled by means of a rotary spring and the outer cylinder being deemed fixed in space. A modal analysis of this oscillating system was conducted, once on the basis of the newly developed method (→ computer run A) and then on the basis of the conventional method stated in /1/, /2/ (→ computer run B), even though the length of the inner cylinder is finite and its motion is not uniform.

Fig. 4 shows the 14 x 14-hydromatrix calculated in run A. It is apparent that even cylinder segments not located on the same y coordinate are under certain circumstances closely coupled by the fluid.

Table I shows the lowest eigenfrequencies. Larger differences evidently occur above eigenfrequency 2 (> 20 %).

eigenfrequencies /Hz/	Run A	Run B	AIR
f_1	8,49	8,55	16,3
f_2	49,6	40,9	75,2
f_3	106	75,5	141

Table I: Eigenfrequencies in air/water for structure shown in fig. 3

For the sake of comparison, the eigenfrequencies for oscillation in air are stated in the right-hand column.

4. Conclusions

The described method of modeling fluid/structure interaction in connection with cylindrical structures can be integrated relatively easily into existing computer codes. It should be used in all instances in the analysis of higher eigenfrequencies in relevant problems.

5. Literature

/1/ R.J. Fritz: The Effect of Liquids on the Dynamic Motions of Immersed Solids, J. of Eng. and Ind., 1972

/2/ E. Kiss: Analysis of the Fundamental Vibration Frequency of a Radial Vane Internal Steam Separator Structure, ANL-7685 Proc. of Conf. on Flow-Induced Vibrations in Reactor System Components, May 1970, Argonne Nat..Lab., Argonne, Illinois

/3/ W.F. Stockey, R.J. Scavuzzo: Normal Mode Solution of Fluid-Coupled Concentric Cylindrical Vessels, Pressure Vessel Technology, Trans. ASME, 100, 350-3 (1978)

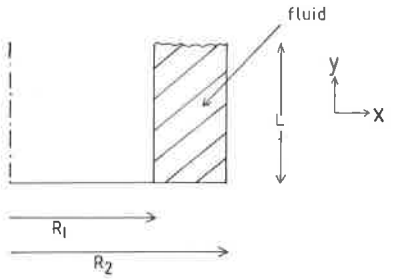

fig. 1: Geometry data for two concentric cylinders

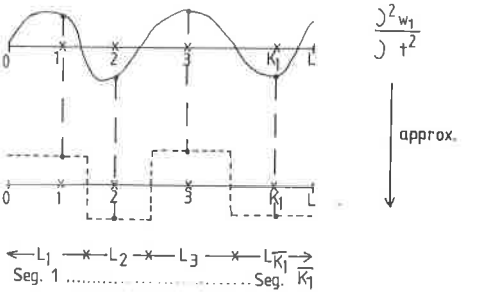

fig. 2: Definition of appropriate cylinder segments

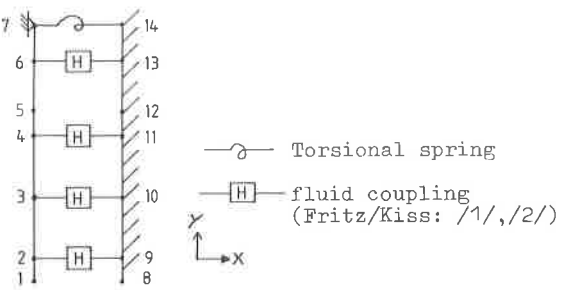

fig. 3: Model Problem

.664396E+04	.154356E+05	.111735E+05	.381722E+04	.181186E+04	.101565E+04	.101803E+03	-.718475E+04
-.176168E+05	-.127895E+05	-.436930E+04	-.207391E+04	-.116255E+04	-.116528E+03		
.154356E+05	.500674E+05	.403591E+05	.139839E+05	.663752E+04	.372072E+04	.372945E+03	-.176168E+05
.558644E+05	-.468319E+05	-.160064E+05	-.759750E+04	-.425885E+04	-.426884E+03		
.111735E+05	.403591E+05	.687733E+05	.299319E+05	.141948E+05	.795701E+04	.797568E+03	-.127095E+05
-.468318E+05	-.766640E+05	-.342097E+05	-.162478E+05	-.910784E+04	-.912921E+03		
.381722E+04	.139839E+05	.299319E+05	.301880E+05	.169581E+05	.949126E+04	.951353E+03	-.436930E+04
-.160064E+05	-.342097E+05	-.331799E+05	-.193596E+05	-.108640E+05	-.108895E+04		
.181186E+04	.663752E+04	.141948E+05	.169581E+05	.195789E+05	.127396E+05	.127431E+04	-.207391E+04
-.759750E+04	-.162478E+05	-.193596E+05	-.212653E+05	-.145309E+05	-.145861E+04		
.101565E+04	.372072E+04	.795701E+04	.949126E+04	.127396E+05	.193116E+05	.258946E+04	-.116255E+04
-.425885E+04	-.910784E+04	-.108640E+05	-.145309E+05	-.206705E+05	-.291309E+04		
.101803E+03	.372945E+03	.797568E+03	.951353E+03	.127431E+04	.258946E+04	.138049E+04	-.116528E+03
-.426884E+03	-.912921E+03	-.108895E+04	-.145861E+04	-.291309E+04	-.104564E+04		
-.718475E+04	-.176168E+05	-.127895E+05	-.436930E+04	-.207391E+04	-.116255E+04	-.116528E+03	.866290E+04
.202190E+05	.146393E+05	.500124E+04	.237386E+04	.133069E+04	.133380E+03		
-.176168E+05	-.558644E+05	-.468318E+05	-.160064E+05	-.759750E+04	-.425885E+04	-.426884E+03	.202190E+05
.654529E+05	.536593E+05	.183214E+05	.869633E+04	.487481E+04	.488625E+03		
-.127895E+05	-.468318E+05	-.766640E+05	-.342097E+05	-.162478E+05	-.910784E+04	-.912921E+03	.146393E+05
.536593E+05	.899004E+05	.392117E+05	.185977E+05	.104251E+05	.104496E+04		
-.436930E+04	-.160064E+05	-.342097E+05	-.331799E+05	-.193596E+05	-.108640E+05	-.108895E+04	.500124E+04
.183214E+05	.392117E+05	.394143E+05	.222138E+05	.124352E+05	.124644E+04		
-.207391E+04	-.759750E+04	-.162478E+05	-.193596E+05	-.212653E+05	-.145309E+05	-.145861E+04	.237386E+04
.869633E+04	.185977E+05	.222138E+05	.255372E+05	.166868E+05	.166957E+04		
-.116255E+04	-.425885E+04	-.910784E+04	-.108640E+05	-.145309E+05	-.206705E+05	-.291309E+04	.133069E+04
.487481E+04	.104251E+05	.124352E+05	.166868E+05	.251583E+05	.338831E+04		
-.116528E+03	-.426884E+03	-.912921E+03	-.108895E+04	-.145861E+04	-.291309E+04	-.104564E+04	.133380E+03
.488625E+03	.104496E+04	.124644E+04	.166957E+04	.338831E+04	.175378E+04		

fig. 4 14 x 14 hydromatrix (rowwise) for example given in fig. 3